Rigid Helical Poly(glycosyl phenyl isocyanide)s: Synthesis, Conformational Analysis, and Recognition by Lectins

Teruaki Hasegawa, Shunsuke Kondoh, Kazunori Matsuura, and Kazukiyo Kobayashi*

Department of Molecular Design and Department of Biotechnology, Graduate School of Engineering, Nagoya University, Chikusa, Nagoya 464-8603, Japan

Received March 25, 1999; Revised Manuscript Received June 28, 1999

ABSTRACT: Glycosylated poly(phenyl isocyanide)s were synthesized in an attempt to elucidate the effect of three-dimensionally regulated saccharide arrays along highly stereoregular polymer backbones on molecular recognition. Poly(phenyl isocyanide)s substituted with α-D-glucose, β-D-glucose, β-D-galactose, and β-lactose were obtained by polymerization of the corresponding acetylated glycosyl phenyl isocyanides with a Ni(II) catalyst and subsequent deacetylation. Helical main chains and spatially regulated saccharide arrays of the poly(phenyl isocyanide)s were demonstrated by CD spectroscopy and molecular dynamics calculations. Their binding affinity with lectins was investigated by inhibition of hemagglutination and fluorescence spectroscopy. The rigid cylindrical phenyl isocyanide glycopolymers exhibited little specific interactions with lectins, which was in contrast to the highly specific interactions of the multivalent glycoclusters along flexible phenylacrylamide glycopolymers. It has been demonstrated that the compatibility of orientation and spacing of clustered saccharide chains of glycopolymers is essential for specific molecular recognition by lectin.

Introduction

Saccharide chains of glycoproteins and glycolipids in cellular surfaces are key substances in various intercellular signal transferring events such as multiplication, adhesion, growth, differentiation, fertilization of cells, and infection with viruses and bacteria.[1−3] Multiantennary or clustered saccharide chains in cellular surfaces are important in the molecular recognitions with carbohydrate-binding proteins.[4−6] The multivalent binding must be achieved, not only via complementarity between individual receptor−ligand pairs but also by controlling the spatial arrangement between individual recognition elements of a multivalent ligand.

Synthetic polymers carrying various kinds of pendent saccharide chains are of interest as a tool to investigate molecular recognition.[7−11] The saccharide chains in these glycopolymers can be attached crowdedly along a polymer backbone, and hence, it is known that the multivalent saccharides enhance protein−carbohydrate interactions significantly.[6,12] We have been engaged in the synthesis and applications of glycosylated polystyrenes, which express strong binding affinities to lectins, viruses, and cells.[13−15] The strong binding may be attributable to the characteristic conformations based on the amphiphilic structural units of glycopolystyrenes. Recently, flexible cylindrical conformations of glycosylated polystyrenes in water have been demonstrated by the small-angle X-ray scattering analysis.[16] Since the oligosaccharide chains are attached to every repeating unit along the hydrophobic polystyrene backbone, the polystyrene backbone is buried inside of the molecule to form a hydrophobic core that is sheltered from water, and hence, the oligosaccharide chains tend to gather on the outside of the polymer in water. It is suggested that the biological functions of glycopolystyrenes have been induced by the highly condensed oligosaccharide chains along the flexible polystyrene backbone.

In these research processes, we are interested in the molecular recognition of three-dimensionally regulated glycopolymers. Although it has been pointed out[12] that not only structural compatibility but also the relative spatial compatibility of oligosaccharides is important for molecular recognition, the effect of the relative spacing of oligosaccharide chains along the glycopolymers on molecular recognition still remains unknown. In this respect, it is important to investigate the molecular recognition of highly stereoregular saccharide arrays. However, the glycosylated polymers investigated so far were not stereoregular and the three-dimensional arrays of the saccharides were not regulated at all.

This paper has focused on the rigid helical conformations of polyisocyanides.[17−24] Glycosylated poly(phenyl isocyanide)s as shown in Chart 1 were prepared by the polymerization of the corresponding phenyl isocyanides substituted with per-*O*-acetyl α-D-glucopyranoside, β-D-glucopyranoside, β-D-galactopyranoside, and β-lactoside. The formation of helix structures is demonstrated by CD spectroscopy and molecular dynamics calculations. The interaction of glycosylated poly(phenyl isocyanide)s with lectins has been investigated by inhibition of hemagglutination and fluorescence spectroscopy. Discussion is made on the molecular recognition of the rigid helical glycopolymers.

Results and Discussion

Synthesis of Glycosylated Poly(phenyl isocyanide)s. The synthetic route of the glycosylated poly(phenyl isocyanide)s is shown in Scheme 1, starting from *p*-nitrophenyl 2,3,4,6-tetra-*O*-acetyl-α-D-glucopyranoside as an example. Hydrogenation of the nitro group to amine followed by formylation with acetic formic anhydride was carried out in ethyl formate. The resulting *N*-formyl-amino group was converted to an isocyano

* Corresponding author. Telephone: +81-52-789-2488. Fax: +81-52-789-2528. E-mail: kobayash@mol.nagoya-u.ac.jp.

10.1021/ma990444j CCC: $18.00
Published on Web 09/08/1999

Chart 1. Rigid Helical Glycosylated Poly(phenyl isocyanide)s

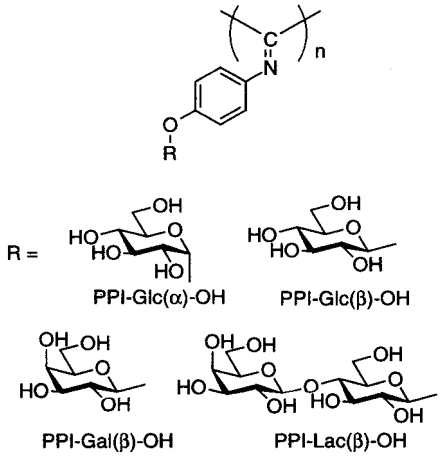

Scheme 1[a]

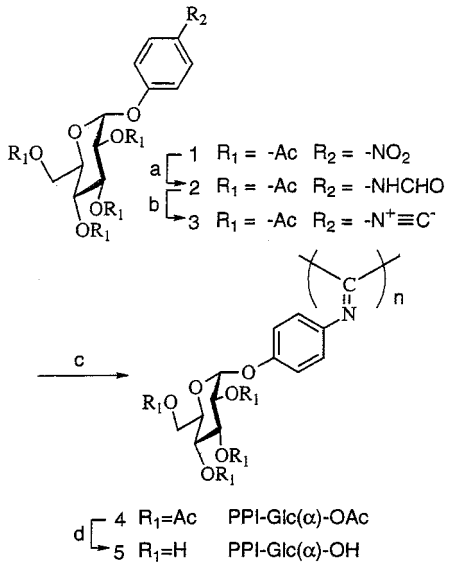

[a] Reagents: (a) H_2, Pd/C, HCOOEt, then HCOOAc, rt, 99%. (b) $POCl_3$, Et_3N, CH_2Cl_2, rt, 68%. (c) $NiCl_2 \cdot 6H_2O$, MeOH, $CHCl_3$, rt, 98%. (d) NaOMe, MeOH, CCl_4, then H_2O, rt, 97%.

group by phosphorus oxychloride and triethylamine. Phenyl isocyanides carrying acetylated β-glucose, β-galactose, and β-lactose were also obtained.

These isocyano derivatives were polymerized with nickel(II) chloride in a mixture of chloroform and methanol as summarized in Table 1. The polymers were soluble in dichloromethane, chloroform, ethyl acetate, dimethylformamide, pyridine, and so on. Their weight-average molecular weights (M_w) determined by light scattering were $(1.5-9.2) \times 10^5$. Their deacetylation with sodium methoxide gave hydroxylated glyco-polyisocyanides which were soluble only in water and dimethyl sulfoxide.

Nolte et al.[18] reported the polymerization of benzoylated α- and β-D-glucopyranosyl isocyanides in which each isocyano group was connected directly to the glucopyranose anomeric carbon. The polymerization of α-anomeric isocyanide was slower than that of β-anomeric isocyanide, and partial isomerization of α-anomeric isocyanide to the β-anomeric one occurred during the polymerization. It was suggested that the anomerization of N-linked α-D-glucopyranoside was caused by the steric repulsion of the axially oriented isocyanide, particularly after being converted to the corresponding polyisocyanide main chain. In the present isocyano derivatives, O-linked D-glycosides are connected to the phenyl aglycon, which is inserted as a spacer. As a result, the steric repulsion is reduced and no anomerization during polymerization was detected.

CD Spectra and Optical Rotations of Glycosylated Poly(phenyl isocyanide)s. Figure 1 illustrates the CD spectra of acetylated and hydroxylated glycopoly(phenyl isocyanide)s, respectively, in chloroform and water. PPI-Glc(α)-OAc induced a negative Cotton effect at 325 nm, while PPI-Glc(α)-OH induced a positive Cotton effect at 280 nm. The other acetylated and hydroxylated PPI-Glc(β), -Gal(β), and -Lac(β) were found to induce a positive Cotton effect. It was reported[17] that negative Cotton effects were assignable to right-handed helical structures of polyisocyanide derivatives, and positive Cotton effects to left-handed helical structures. The present glycopolyisocyanides, except PPI-Glc(α)-OAc, were spatially regulated in left-handed helical structures. It is noteworthy that the right-handed helix of PPI-Glc(α)-OAc was inverted to the left-handed helix of PPI-Glc(α)-OH by the deacetylation procedure.

The helix inversion was also supported by their optical rotations. It was reported[25] that the negative and positive shifts of the optical rotations by polymerization were respectively assignable to the formation of the right- and left-handed helical conformation of polyisocyanide backbones. The optical rotation (+68.3°) of PPI-Glc(α)-OAc was shifted negatively from that of its monomer (+166.8°) by polymerization. On the other hand, the rotation of PPI-Glc(α)-OH (+261.9°) was shifted positively from that of its hypothetical monomeric compound (*p*-isocyanophenyl α-D-glucopyranoside, +150.6°).

Computer Simulations of Glycosylated Poly(phenyl isocyanide)s. The calculations of molecular mechanics and molecular dynamics were carried out using Insight II/Discover programs and pcff force fields.[26-28] The structures of the side chain and main chain of glycosylated phenyl isocyanides were optimized by molecular mechanics, and then the decamers of the glycosylated phenyl isocyanides were optimized by molecular dynamics simulations.

Figure 2 illustrates the potential energy maps for the hypothetical side chain models. The conformations of glycoside linkages were defined by the two dihedral angles (ϕ and φ). The minimum potential energies were observed at $\phi = 86.0°$ and $\varphi = 169.2°$ for the Glc(α)-OH model and at $\phi = 77.4°$ and $\varphi = 172.1°$ for the Glc(α)-OAc model. The most stable conformation of the side chain structure of the Glc(α)-OH model is shown in Figure 3. It can be seen that the phenyl aglycon is perpendicular to the glucopyranose ring plane, probably to minimize their steric repulsion.

Figure 4 plots the potential energies of the optimized conformation of PPI-Glc(α)-OH (DP = 8) against the dihedral angles (Φ_0) of the main chain at 10° intervals. The most stable left-handed helix and right-handed helix were obtained at $\Phi_0 = -140°$ and 120°, respectively, and the left-handed helix was more stable than the right-handed one. PPI-Glc(α)-OAc (DP = 8) also exhibited a similar energy profile, but the right-handed helical conformation ($\Phi_0 = 140°$) was the most stable one. It is suggestive of the preference of the left- and

Table 1. Polymerization of Glycosylated Phenyl Isocyanides by Ni Catalyst[a]

glycosylated poly(phenyl isocyanide)s	monomer, g (mmol)	$NiCl_2 \cdot 6H_2O$, mg (μmol)	solvent, [b] mL	time, h	yield, %	M_w[c] $\times 10^{-5}$
PIP-Glc(α)-OAc	0.11(0.24)	4.18(17.6)	0.8	48	85	–
	1.66(3.56)	2.25(9.47)	8.0	58	98	1.5
	2.21(4.90)	2.02(8.50)	10.0	48	98	1.8
	0.38(0.86)	14.3(60.2)	20.0	29	41	–
PIP-Glc(*β*)OAc	2.67(5.89)	3.01(12.7)	60.0	31	63	1.6
PIP-Gal(*β*)-OAc	0.48(1.07)	0.10(0.42)	13.0	48	56	7.1
PIP-Lac(*β*)OAc	0.35(0.45)	0.10(0.42)	5.0	144	55	9.2

[a] At room temperature. [b] Chloroform−methanol = 1:1 in volume. [c] Determined by light scattering in chloroform as solvent.

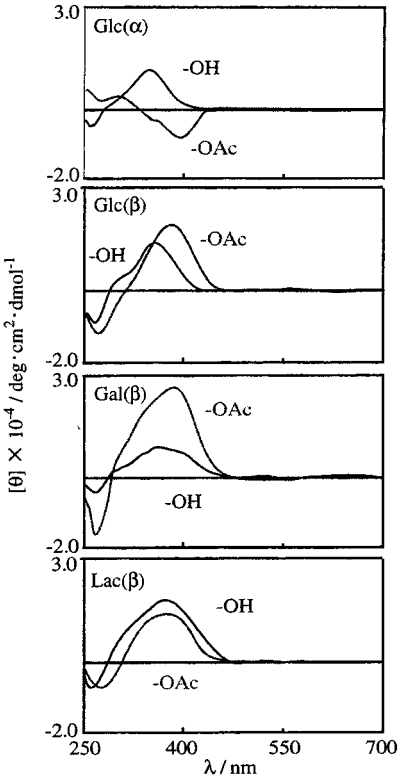

Figure 1. CD spectra of poly(phenyl isocyanide)s bearing acetylated (OAc) and hydroxylated (OH) glycosides.

right-handed helical conformation of PPI-Glc(α)-OH and -OAc, respectively.

Molecular dynamics calculations were performed using the decamers with the optimized helical and side chain conformations as the initial structures. To approach the real conformation and its stability at room temperature, 500 ps molecular dynamics calculation was performed at 300 K with use of the dielectric constant $\epsilon = 1.0$ after energy minimization and 100 ps equilibrium. The time courses of the dihedral angle (Φ_0) of the main chain structure are shown in Figure 5. The dihedral angles between the terminal 1 and 2 residues and between the terminal 9 and 10 residues rapidly converged to 0° and 180°, respectively. However, the other linkages of both the left- and right-handed helixes retained their initial dihedral angles during the observed time courses. The fixed dihedral angle is strong evidence of the structural rigidity of the glycopolyisocyanide helixes.

Figure 6 illustrates the rodlike conformations of polyisocyanide (DP = 30) bearing the acetylated and hydroxylated α-glucose moieties obtained by the molecular dynamics run. The diameters of the acetylated and hydroxylated forms were about 24 and 20 Å, respectively. The helix becomes more slender and more stretched than the one estimated from 4_1 helixes reported for the other polyisocyanides.[24] That is probably due to the steric repultion among the highly crowded, bulky saccharide chains.

Table 2 summarizes the average potential energies per residue of PPI-Glc(α) and PPI-Glc(*β*) estimated by the molecular dynamics. The left-handed structures were more stable for PPI-Glc(α)-OH, PPI-Glc(*β*)-OAc, and PPI-Glc(*β*)-OH than the right-handed ones. In contrast, for PPI-Glc(α)-OAc, the right-handed helix was more stable than the left-handed one. The right-handed helix of PPI-Glc(α)-OAc was inversed by deacetylation to the left-handed helix of PPI-Glc(α)-OH. The helix senses of glycopolymers predicted by molecular dynamics were consistent with those determined by the CD spectroscopy.

Helix senses of the acetylated and hydroxylated glycopolyisocyanides can be discussed as follows. A dominant factor to determine the helix senses of helical polymers with side chain chiral centers is the chirality at the position closest to the polyisocyanide main chain. The chirality of the anomeric center is the most important for helix sense in acetylated glyco-polyisocyanides. The opposite chirality of the anomer position is reflected as the opposite helix senses of PPI-Glc(α)-OAc and PPI-Glc(*β*)-OAc. On the other hand, the molecular dynamics calculations showed that hydrogen-bond networks were extended among the free carbohydrates of PPI-Glc(α)-OH and PPI-Glc(*β*)-OH. We assumed that the hydrogen-bond networks became more dominant to stabilize the helical conformation of hydroxylated glyco-polyisocyanides, and as the results, the right-handed helix of PPI-Glc(α)-OAc was inversed to the left-handed helix of PPI-Glc(α)-OH.

Recognition of Glycosylated Poly(phenyl isocyanide)s with Lectins. The binding affinity of the glycopolymers with lectins was investigated by inhibition of hemagglutination and fluorescence spectroscopy using RCA_{120} (*Ricinus communis* agglutinin from castor bean) and ConA (concanavalin A from jack bean). Figure 7 illustrates the minimum inhibition concentrations (IC_{min}) to inhibit lectin-induced hemagglutination. Flexible glycosylated poly(acryloylaminophenyl) derivatives[29] (abbreviated as PAP) and low molecular weight *p*-nitrophenyl glycosides (abbreviated as pNP) were used for comparison. IC_{min} of PPI-Gal(*β*) for RCA_{120}-induced hemagglutination was 1.9×10^{-5} M. Despite the polyvalency of PPI-Gal(*β*), the IC_{min} was similar to that of a monovalent ligand or galactose itself and also to that for ConA-induced hemagglutination. The specificity of PPI-type glycopolymers was not detected. This is quite in contrast to the observation that PAP-Gal(*β*) exhibited a specific and higher inhibition ability (1.3×10^{-7} M), which was 200 times stronger than that of galactose itself and 10 times stronger than that of pNP-Gal(*β*).

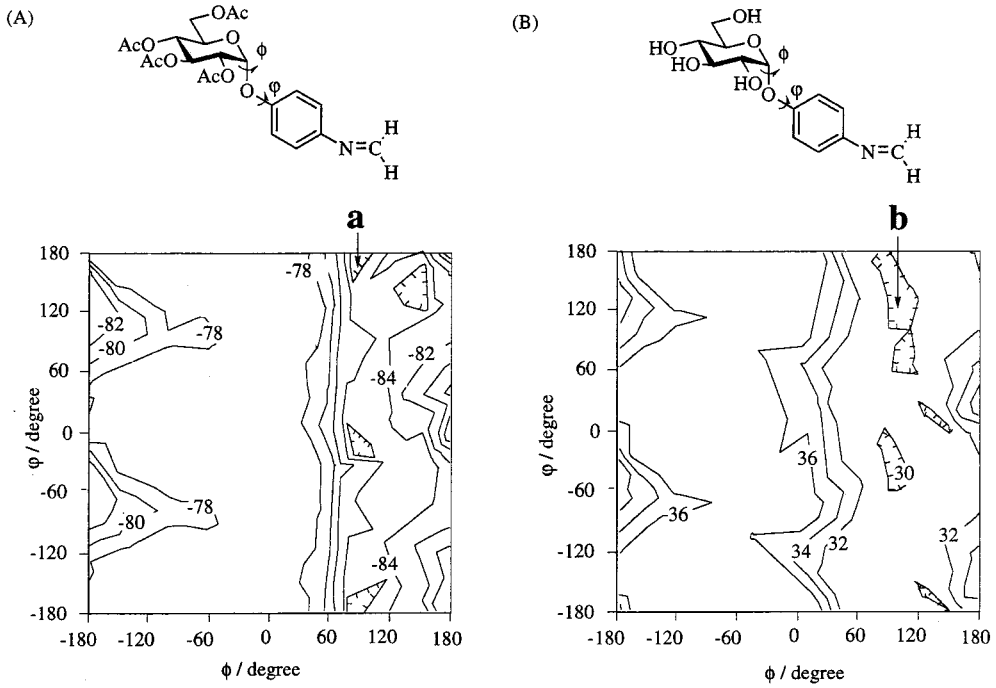

Figure 2. Contour maps of the potential energy surface in $\phi-\varphi$ space for side chain model bearing (A) acetylated and (B) hydroxylated α-glucose moieties. Each potential well is indicated by a and b. The contour interval is 2 kcal mol^{-1}.

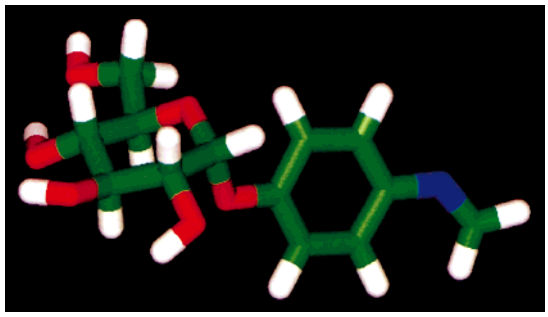

Figure 3. The most stable conformation of the side chain model of the Glc(α)-OH.

The nonspecific interaction of rigid PPI-type polymers, in contrast to the enhanced affinity and specificity of the flexible PAP-type glycopolymers, was also demonstrated by fluorescence spectroscopy using FITC-labeled RCA_{120} and ConA. The fluorescence intensity of FITC-labeled RCA_{120} was decreased with addition of these glycopolymers. The relative change of fluorescence intensity ($\Delta F/F_0$) at 518 nm is plotted against the sugar concentration in Figure 8a. As shown in Figure 8b, the plots of [sugar]$F_0/\Delta F$ vs [sugar] gave a linear relationship, in accordance with the eq 1. The binding constants

$$\frac{[\text{sugar}]F_0}{\Delta F} = \frac{[\text{sugar}]F_0}{\Delta F_{\max}} + \frac{F_0}{\Delta F_{\max} K_a} \qquad (1)$$

(K_a) of the glycopolymers to the lectin were estimated from the slopes and intercepts and are shown in Figure 9.

The binding constants of the specific combinations of PAP-Glc(α)/ConA, PAP-Gal(β)/RCA_{120}, and also PAP-Lac(β)/RCA_{120} were on the order of 10^6-10^7 M^{-1}, and those of the other nonspecific combinations of PAP-type polymers were on the order of 10^4 M^{-1}. On the other hand, all of the binding constants of PPI-type glycopolymers to FITC−RCA_{120} and FITC−ConA were on the order of 10^4 M^{-1}, indicating again that PPI-type glycopolymers did not exhibit specific bindig to these lectins.

The nonspecific interaction of the PPI glycopolymers for the lectins may be ascribed to the crowded saccharide arrays along the rigid cylindrical polymer backbone. The saccharide arrays are crowded too thickly to be accessible or to be induced-fit to the binding sites. The evidence comes from the molecular dynamic calculations suggesting that the intramolecular hydrogen-bond networks are extended among the saccharide chains. In contrast, the saccharide chains of the PAP-Gal(β) are also crowded, but they are flexible enough to be induced-fit to the binding sites of the lectins. The multivalent binding can be achieved by the compatible orientations and spacing of the saccharide chains along the flexible glycopolymers.

The influence of saccharide density along the glycopolymers has been investigated using their copolymers. *p*-Isocyanophenol was selected as a comonomer of *p*-isocyanophenyl α-D-glucopyranoside to retain the rigid rodlike polymer backbone. Acrylamide was copolymerized with *p*-acryloylaminophenyl α-D-glucopyranoside to retain the flexible polymer backbone. The binding constants between FITC−ConA and these copolymers were estimated in the same way and are shown in Figure 10. The binding constants were increased by inserting the respective comonomers. The rigid PPI glycopolymer with a mole fraction of 0.41 gave $K_a = 1.1 \times 10^6$ M^{-1}, which was about 40 times that of the rigid homopolymer. The flexible copolymer with the mole fraction of 0.58 gave $K_a = 1.1 \times 10^8$ M^{-1}, which was about 10 times that of the flexible homopolymer. The effects of copolymerization on binding affinities are more clearly detected in rigid glycopolymers, but the association constant of the rigid copolymer was only about 10^{-2} times that of the flexible copolymer.

A higher affinity for copolymers is often encountered in binding to lectins. All of the saccharide chains along the polymer backbone cannot necessarily bind to the

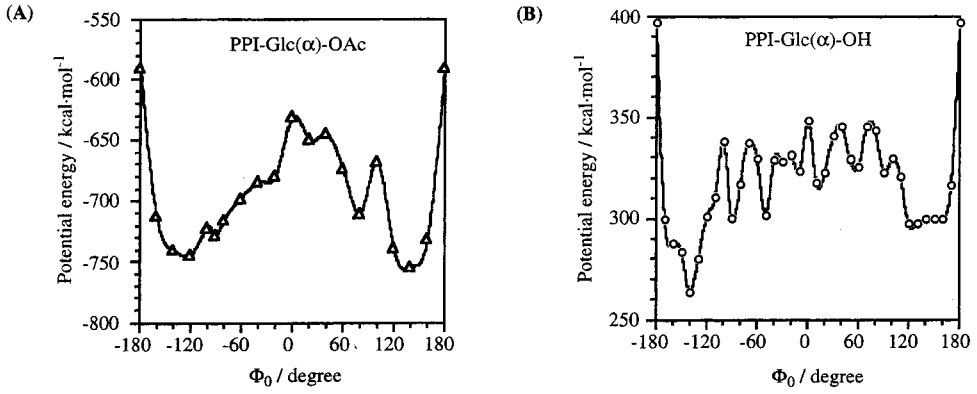

Figure 4. Potential energy of (A) PPI-Glc(α)-OAc and (B) PPI-Glc(α)-OH (DP = 8) after minimization.

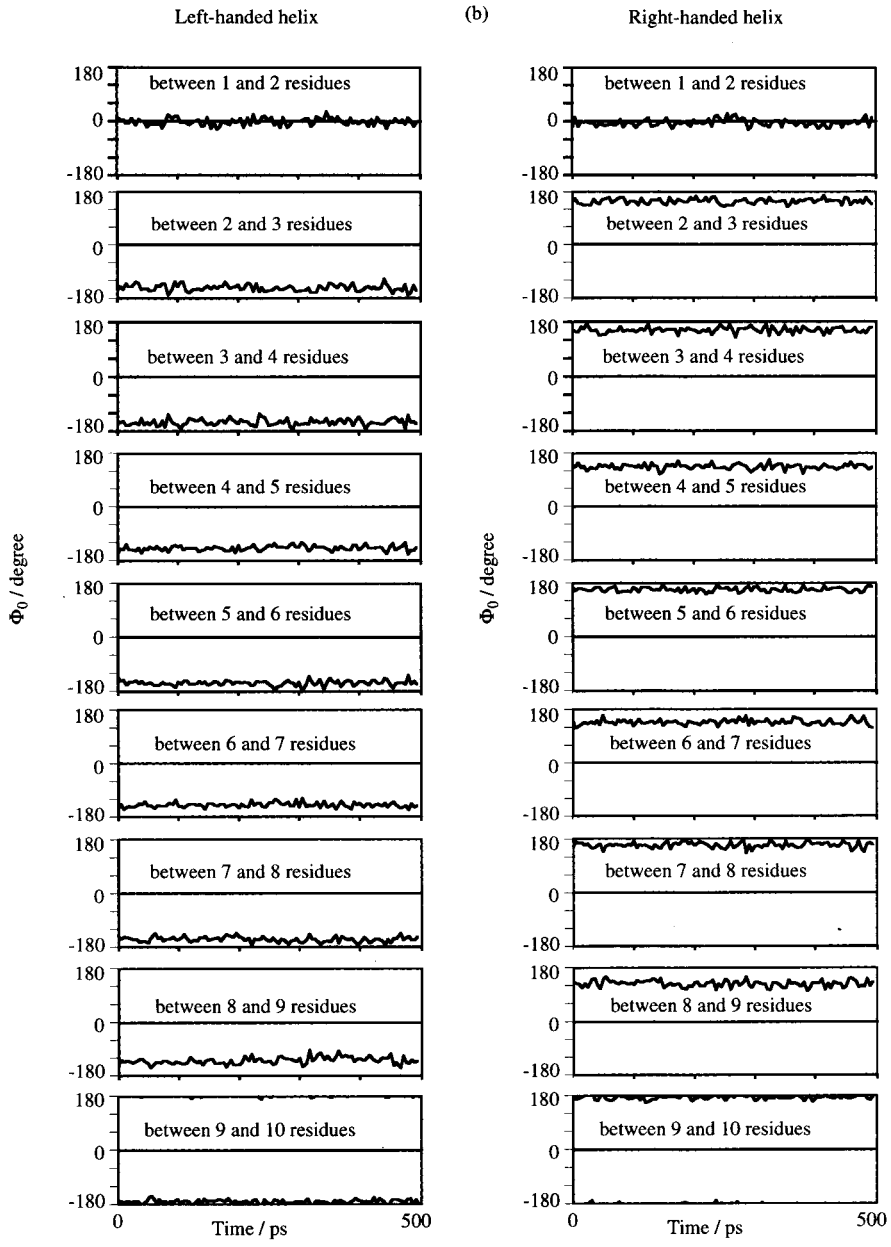

Figure 5. History of dihedral angles of PPI-Glc(α)-OH (DP = 10). The initial structures for molecular dynamics calculation were (a) left- and (b) right-handed helix, respectively.

binding sites, and hence an unavailable or excess amount of saccharide chains are buried in the polymers, especially in the homopolymers. However, unavailable saccharide chains are decreased in copolymers, which results in an increase of the apparent binding affinity of the copolymers.

Insertion of the comonomer units into the rigid PPI glycopolymer backbone was found to increase the bind-

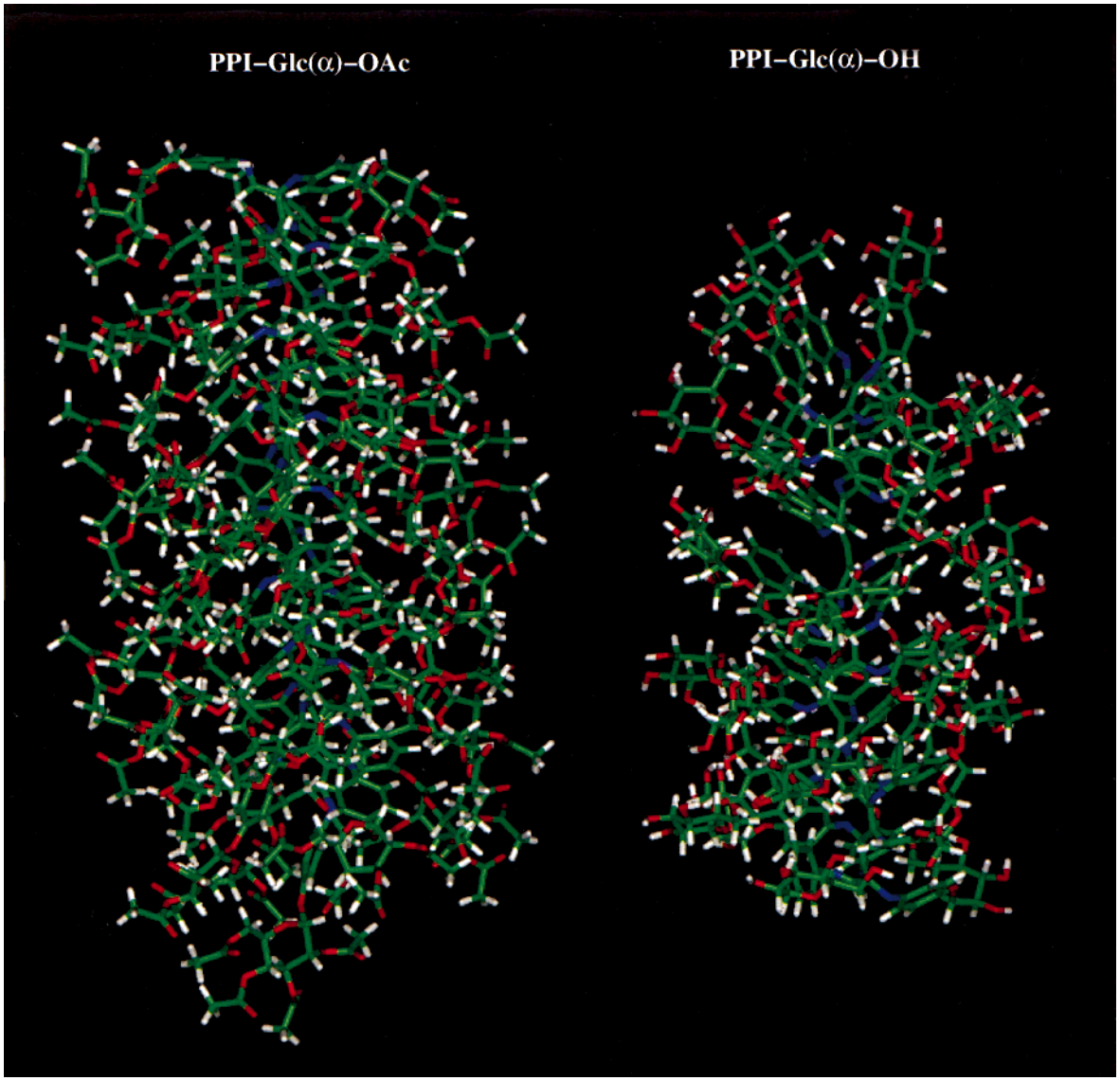

Figure 6. Snapshots of PPI-Glc(α)-OAc (left) and -OH (right), (DP = 30), at 500 ps dynamics.

Table 2. Average Potential Energy of Polyisocyanides bearing α- and *β*-Glucose Moieties

	potential energy (kcal/mol$_{res}$)		helix sense	
	right	left	MD[a]	CD[b]
PIP-Glc(α)				
−Ac	−33.6 ± 0.9	−34.0 ± 0.8	right	right
−OH	65.6 ± 0.6	65.9 ± 0.7	left	left
PIP-Glc(*β*)				
−Ac	−57.9 ± 0.8	−56.1 ± 0.7	left	left
−OH	65.1 ± 0.6	65.4 ± 0.6	left	left

Helix senses were estimated by [a]molecular dynamics or [b]CD spectroscopy.

ing affinity to the lectin. The induced-fitting of the saccharide chains was facilitated by the separation of the neighboring saccharide chains and also by the releasing of the intramoleculer hydrogen-bond networks. However, the affinity of PPI-type copolymers was still lower than that of the flexible PAP-type copolymers. The rigidity of the PPI polymer backbone is still resistant to the spacial arrangement of the saccharides chains to be induced-fit to the binding sites.

In conclusion, the incompatibility between thickly crowded saccharide arrays along a rigid rodlike polymer backbone and the carbohydrate binding sites of lectins has been clearly detected in this work. As far as we know, this is the first example of the incompatible relative orientations or spacing of saccharide units in the multivalent arrays, although the concept was previously pointed out. It is important to note that the flexibility of the saccharide chains and also of the polymeric backbone plays an important role in enhancing affinities between glycopolymers and lectins. These rigid cylindrical glycopolymers exhibited characteristic adsorption behaviors and self-organization onto hydrophilic surfaces, which will be reported elsewhere.

Experimental Section

General Methods. ^{1}H NMR and ^{13}C NMR spectra were recorded on Varian Gemini-200 and Gemini-500 NMR spectrometers. The chemical shifts are reported in ppm (*δ*) relative to Me_4Si or residual nondeuterated solvents. IR spectra was recorded on a JASCO FT/IR-230 Fourier transform infrared spectrometer. Optical rotations were determined with a JASCO DIP-1000 digital polarimeter using a water-jacketed 100 mm cell at 25 °C. Weight-average moleculer weight of polymers were determined on a DAWN DSP−F multiangle laser light scattering photometer (Wyatt Technology). Circular dichroism spectroscopy (CD) was carried out with a JASCO J-720L spectropolarimeter using a 10 mm cell. Fluorescence spectroscopy was carried out with a JASCO FP-777 spectro-

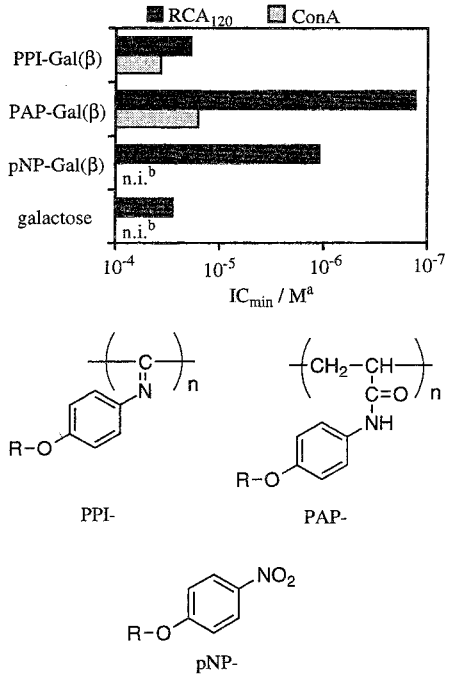

Figure 7. Minimum inhibitory concentration (IC_{min}) of glycopolymers to inhibit lectin-induced hemagglutination. [Lectin] = 4 × (minimum concentration require for hemagglutination). [a]Molarity of the saccharide unit. [b]n.i., not inhibited by 1.0×10^{-4} M.

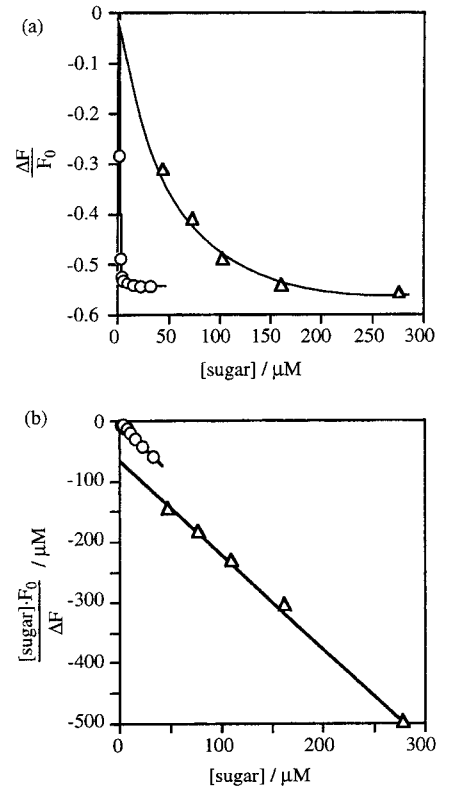

Figure 8. (a) Quenching of fluorescence intensities by addition of PPI-Gal(β) (Δ), and PAP-Gal(β) (○). (b) The linearized plot. The concentration of FITC-labeled RCA_{120} was 40 μM. ex = 490 nm, at 25 °C.

fluorometer. Molecular mechanics and molecular dynamics calculations were carried out using the Insight II/Discover program at Venture Business Laboratory of Nagoya University. Silica gel 60 (particle size 0.063−0.200 mm) for chromatography was purchased from Merck. Thin-layer chromatography (TLC) was carried out with Merck TLC plates precoated with silica gel 60. Lectin-binding assays were carried out by inhibition of hemagglutination[30] and fluorescence spectroscopy.[31,32] ConA and RCA_{120} were purchased from Sigma.

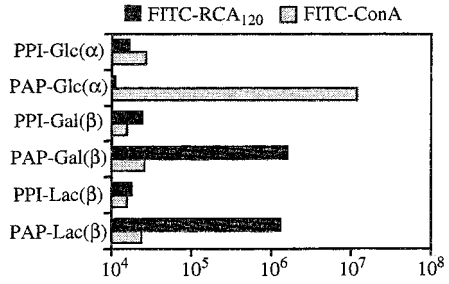

Figure 9. Association constants between glycopolymers and FITC-labeled lectins.

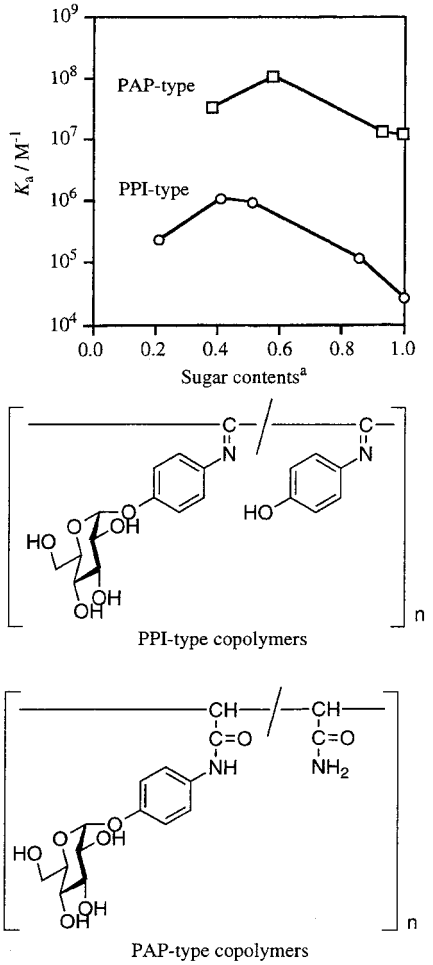

Figure 10. Association constants between PPI-type (O) and PAP-type (□) copolymers. [a] The mole fraction of the saccharide-carrying monomeric unit.

***p*-*N*-Formylaminophenyl 2,3,4,6-Tetra-*O*-acetyl-α-D-glucopyranoside (2).** *p*-Nitrophenyl 2,3,4,6-tetra-*O*-acetyl-α-D-glucopyranoside (**1**) (8.51 g, 18.1 mmol) was dissolved in 100 mL of ethyl formate, and then 10% palladium on carbon (0.43 g) was added. The mixture was bubbled with hydrogen gas with stirring at room temperature for 30 min until TLC (ethyl acetate−hexane, 3:2) indicated complete conversion of **1**. The catalytic palladium on carbon was removed by filtration, and acetic formic anhydride (3 mL, 37 mmol) was added to the resulting solution. Stirring was continued for 10 min, and the resulting solution was poured into an ice-cold saturated sodium bicarbonate aqueous solution. The organic layer was washed with a saturated sodium bicarbonate solution, dried

over anhydrous magnesium sulfate, and evaporated in dryness. The product was purified by chromatograghy on a silica gel column (30 cm long, 3 cm i.d., chloroform−methanol = 25:1 in v/v) to give 2.24 g (99.5%) of **2** as a colorless solid: mp 103.5−104.5 °C; $[\alpha]^{25}_D$ +141.2° (*c* 1.0, $CHCl_3$); ^{1}H NMR (500 MHz, $CDCl_3$) δ 8.57 (d, J = 11.5 Hz, formyl-trans), 8.34 (d, J = 2.0 Hz, formyl-cis), 8.05 (d, J = 11.5 Hz, amide-trans), 7.59 (br s, amide-trans), 7.49 (d, J = 9.0 Hz, 2H, phenyl-cis), 7.43 (d, J = 1.5 Hz, phenyl-trans), 7.06 (d, J = 9.5 Hz, phenyl-cis), 7.04 (d, J = 10.0 Hz, phenyl-trans), 5.76−5.62 (m, H-1 and H-3), 5.17 (dd, J = 10.0 and 10.0 Hz, H-4-cis), 5.16 (dd, J = 10.0 and 10.0 Hz, H-4-trans), 5.04 (dd, J = 3.5 and 10.5 Hz, H-2-cis), 5.03 (dd, J = 3.5 and 10.5 Hz, H-2-trans), 4.26 (dd, J = 4.5 and 12.5 Hz, H-6R-trans), 4.25 (dd, J = 4.5 and 12.5 Hz, H-6R-cis), 4.14−4.09 (m, 1H, H-5), 4.07 (dd, J = 2.5 and 12.5 Hz, 1H, H-6S-cis), 4.06 (dd, J = 2.5 and 12.5 Hz, H-6S-trans), and 2.10−2.03 (m, 12H, acetyl), (cis/trans = 1.45); ^{13}C NMR (500 MHz, $CDCl_3$) δ 170.51, 170.45, 170.12, 170.11, 169.54, 169.50, 168.31, and 168.30 (C═O, acetyl), 162.51 and 158.85 (C═O, amide), 152.92, 152.66, 132.20, 131.87, 121.64, 121.53, 117.14, and 117.06 (phenyl), 94.57 and 94.54 (C-1), 70.40 and 70.39 (C-2), 69.97 and 69.89 (C-3), 68.27 and 68.21 (C-4), 67.99 and 67.95 (C-5), 61.55 and 61.52 (C-6), and 20.64, 20.64, 20.61, 20.60, 20.56, 20.56, 20.53, and 20.52 (CH_3, acetyl); IR (KBr, cm^{-1}) 3352 (ν_{N-H}), 1753 ($\nu_{C=O}$ acetyl), and 1695 ($\nu_{C=O}$ formyl), 1514 (δ_{N-H}), and 1219 (ν_{C-O}); MS *m*/*z* 551 (MH^+).

***p*-*N*-Formylaminophenyl 2,3,4,6-tetra-*O*-acetyl-*β*-D-glucopyranoside:** ^{1}H NMR (200 MHz, $CDCl_3$) δ 8.62 (d, J = 11.5 Hz, formyl-trans), 8.34 (d, J = 2.0 Hz, formyl-cis), 8.10 (d, J = 11.5 Hz, amide-trans), 7.66 (br s, amide-trans), 7.48 (d, J = 9.0 Hz, 2H, phenyl), 6.98 (d, J = 9.0 Hz, 2H, phenyl), 5.36−5.00 (m, 4H, H-1,2,3,4), 4.30 (dd, J = 5.0 and 12.4 Hz, 1H, H-6R), 4.30 (dd, J = 5.0 and 12.4 Hz, 1H, H-6S), 5.17 (dd, J = 9.7 and 9.7 Hz, 1H, H-4), 5.05 (m, 1H, H-6$_S$), 3.90−3.79 (m, 1H, H-5), and 2.09, 2.07, 2.05, and 2.04 (m, 12H, acetyl).

***p*-*N*-Formylaminophenyl 2,3,4,6-tetra-*O*-acetyl-*β*-D-galactopyranoside:** ^{1}H NMR (200 MHz, $CDCl_3$) δ 8.47 (d, J = 11.5 Hz, formyl-trans), 8.34 (d, J = 2.0 Hz, formyl-cis), 8.01 (d, J = 11.5 Hz, amide-trans), 7.88 (br s, amide-trans), 7.49 (d, J = 8.8 Hz, 2H, phenyl), 6.99 (d, J = 9.0 Hz, 2H, phenyl), 5.48 (dd, J = 7.8 and 10.4 Hz, 1H, H-2), 5.46 (m, 1H, H-4), 5.10 (dd, J = 3.4 and 10.4 Hz, 1H, H-3), 4.98 (δ, J = 7.8 Hz, 1H, H-1), 4.30−4.00 (m, 3H, H-5 and H-6), and 2.30−2.00 (m, 12H, acetyl); IR (KBr, cm^{-1}) 1751 ($\nu_{C=O}$ acetyl), and 1687 ($\nu_{C=O}$ formyl), and 1540 (δ_{N-H}).

***p*-*N*-Formylaminophenyl 2,3,4,6-tetra-*O*-acetyl-*β*-lactoside:** ^{1}H NMR (200 MHz, $CDCl_3$) δ 7.48 (d, J = 9.0 Hz, 2H, phenyl), 7.00 (d, J = 9.0 Hz, 2H, phenyl), 5.37 (m, 1H, H-4′), 5.34−5.05 (m, 3H, H-2, 3, and 2′), 5.21 (d, J = 8.0 Hz, 1H, H-1), 5.07 (dd, J = 3.4 and 10.6 Hz, 1H, H-3′), 4.52 (d, J = 8.0 Hz, 1H, H-1′), 4.30−4.10 (m, 4H, H-4, H-5′, and H-6′), 4.00−3.80 (m, 3H, H-5 and H-6), and 2.30−2.00 (m, 21H, acetyl); IR (KBr, cm^{-1}) 2127 (ν_{NC}) and 1754 ($\nu_{C=O}$ acetyl).

***p*-Isocyanophenyl 2,3,4,6-Tetra-*O*-acetyl-α-D-glucopyranoside (3).** Phosphorus oxychloride (2.0 mL) was added to a solution of 2.24 g (4.94 mmol) of **2** in triethylamine (40 mL) and dichloromethane (10 mL) at 0 °C with magnetic stirring. The mixture was stirred at room temperature until TLC (chloroform−methanol = 25:1) indicated complete conversion. The mixture was poured into an ice-cold saturated sodium bicarbonate aqueous solution. The organic layer was separated and the aqueous layer was extracted five times with dichloromethane. The combined organic layer was dried overnight over anhydrous magnesium sulfate and concentrated in an evaporator to dryness. The product was separated by chromatograghy on a silica gel column (30 cm long, 3 cm i.d., chloroform−methanol = 25:1 in volume) to give 1.67 g (77.7%) of **4** in a colorless solid: $[\alpha]^{25}_D$ +166.8° (*c* 1.0, $CHCl_3$); ^{1}H NMR (200 MHz, $CDCl_3$) δ 7.37 (d, J = 9.0 Hz, 2H, phenyl), 7.11 (d, J = 9.0 Hz, 2H, phenyl), 5.86 (d, 1H, H-1), 5.68 (dd, J = 9.9 and 9.9 Hz, 1H, H-3), 5.17 (dd, J = 9.7 and 9.7 Hz, 1H, H-4), 5.05(dd, J = 3.8 and 10.3 Hz, 1H, H-2), 4.30−4.00 (m, 3H, H-5 and H-6), and 2.00−2.10 (m, 12H, acetyl); ^{13}C NMR (200 MHz, $CDCl_3$) δ 170.48, 170.19, 170.18, and 169.58 (C═O, acetyl), 163.84, 156.18, 127.88, and 117.20 (phenyl), 121.51 (isocyano), 94.04 (C-1), 69.96 (C-2), 69.51 (C-3), 68.14 (C-4), 67.84 (C-5), 61.21 (C-6), 20.32, 20.29, 20.25, and 20.23 (CH_3, acetyl); IR (KBr, cm^{-1}) 2126 (ν_{NC}) and 1753($\nu_{C=O}$ acetyl).

***p*-Isocyanophenyl 2,3,4,6-Tetra-*O*-acetyl-*β*-D-glucopyranoside:** ^{1}H NMR (200 MHz, $CDCl_3$) δ 7.32 (d, J = 9.0 Hz, 2H, phenyl), 6.99 (d, J = 9.0 Hz, 2H, phenyl), 5.35−5.08 (m, 4H, H-1, H-2, H-3, and H-4), 4.05−4.03 (m, 2H, H-5 and H-6$_R$), 3.92−3.82 (m, 1H, H-6$_R$), and 2.10−2.00 (m, 12H, acetyl); IR (KBr, cm^{-1}) 2123 (ν_{NC}) and 1745($\nu_{C=O}$ acetyl).

***p*-Isocyanophenyl 2,3,4,6-tetra-*O*-acetyl-*β*-D-galactopyranoside:** ^{1}H NMR (200 MHz, $CDCl_3$) δ 7.34 (d, J = 9.0 Hz, 2H, phenyl), 7.00 (d, J = 9.0 Hz, 2H, phenyl), 5.60−5.40 (m, 2H, H-2 and 4), 5.11 (dd, J = 3.4 and 10.6 Hz, 1H, H-3), 5.07 (d, J = 7.8 Hz, 1H, H-1), 4.30−4.00 (m, 3H, H-5 and H-6), and 2.30−2.00 (m, 12H, acetyl); IR (KBr, cm^{-1}) 2127(ν_{NC}) and 1752-($\nu_{C=O}$ acetyl).

***p*-Isocyanophenyl 2,3,6,2′,3′,4′,6′-hepta-*O*-acetyl-*β*-lactoside:** $[\alpha]^{25}_D$ −23.7° (*c* 0.5, $CHCl_3$); ^{1}H NMR (200 MHz, $CDCl_3$) δ 7.33 (d, J = 9.0 Hz, 2H, phenyl), 6.97 (d, J = 9.0 Hz, 2H, phenyl), 5.37−5.05 (m, 6H, H-1, H-2, H-3, H-2′, H-3′, and H-4′), 4.60−4.43 (m, 2H, H-1′, H-6R), 4.20−3.70 (m, 6H, H-4, H-5, H-6S, H-5′, and H-6′), and 2.30−2.00 (m, 21H, acetyl); IR (KBr, cm^{-1}) 2127 (ν_{NC}) and 1754 ($\nu_{C=O}$ acetyl).

Poly(*p*-isocyanophenyl 2,3,4,6-tetra-*O*-acetyl-α-D-glucopyranoside) (4). To a solution of 1.66 g (3.55 mmol) of **3** in 4.0 mL of chloroform and 4.0 mL of methanol was added 1.9 mg of nickel(II) chloride hexahydrate. The mixture was stirred at room temperature for 2 days and poured into a mixture of 800 mL of methanol and 200 mL of water. The precipitate was isolated by filtration and dried in vacuo, yielding 1.63 g (98%) of **4** in a brown solid: $[\alpha]^{25}_D$ +68.3° (*c* 1.0, $CHCl_3$); ^{1}H NMR (500 MHz, $CDCl_3$, 50 °C) δ 6.5 (br, phenyl), 5.5, 5.1, and 4.0 (br, sugar moiety), 2.0 (br, acetyl); IR (KBr, cm^{-1}) 1747 ($\nu_{C=O}$) and 1640 ($\nu_{N=C}$).

Poly(*p*-isocyanophenyl 2,3,4,6-tetra-*O*-acetyl-*β*-D-glucopyranoside): ^{1}H NMR (500 MHz, $CDCl_3$, 50 °C) δ 6.5 (br, phenyl), 5.6, 5.4, and 4.6 (br, sugar moiety), 2.0 (br, acetyl); IR (KBr, cm^{-1}) 1755 ($\nu_{C=O}$) and 1638 ($\nu_{N=C}$).

Poly(*p*-isocyanophenyl 2,3,4,6-tetra-*O*-acetyl-*β*-D-galactopyranoside): ^{1}H NMR (500 MHz, $CDCl_3$, 50 °C) δ 6.5 (br, phenyl), 5.4, 5.1, and 4.1 (br, sugar moiety), 2.0 (br, acetyl); IR (KBr, cm^{-1}) 1752 ($\nu_{C=O}$) and 1637 ($\nu_{N=C}$).

Poly(*p*-isocyanophenyl 2,3,6,2′,3′,4′,6′-hepta-*O*-acetyl-*β*-lactoside): $[\alpha]^{25}_D$ +92.2° (*c* 0.7, $CHCl_3$); ^{1}H NMR (500 MHz, $CDCl_3$, 50 °C) δ 6.4 (br, phenyl), 5.4, 5.1, and 4.1 (br, sugar moiety), 2.0 (br, acetyl); IR (KBr, cm^{-1}) 1751 ($\nu_{C=O}$) and 1639 ($\nu_{N=C}$).

Poly(*p*-isocyanophenyl-α-D-glucopyranoside) (5). The polymer **4** (1.00 g, 2.30 mmol) was dissolved in a mixture of methanol, tetrahydrofuran, and tetrachloromethane (1:2:2, 500 mL). A catalytic amount of sodium methoxide (45 mg) was added and the solution was stirred at room temperature for 30 min. Water (200 mL) was added to dissolve a precipitate. The organic layer was evaporated and the remaining aqueous solution was stirred for 2 h. The solution was concentrated, dialyzed in a cellulose dialyzer tube VT801 (cutoff 6000−8000) against water for 2 days, and lyophilized to give 0.60 g (93.5%) of a yellow solid (**5**): $[\alpha]^{25}_D$ +261.9° (*c* 1.0, H_2O); ^{1}H NMR (500 MHz, D_2O, 50 °C) δ 6.7(br, phenyl), 5.7, 5.3, and 4.6 (br, m, sugar); IR (KBr, cm^{-1}) 3430 (ν_{O-H}).

Poly(*p*-isocyanophenyl *β*-D-glucopyranoside): ^{1}H NMR (500 MHz, D_2O, 50 °C) δ 6.9 (br, phenyl), 5.9, 5.6, and 4.3 (br, m, sugar); IR (KBr, cm^{-1}) 3430 (ν_{O-H}).

Poly(*p*-isocyanophenyl *β*-D-galactopyranoside): ^{1}H NMR (500 MHz, D_2O, 50 °C) δ 6.8 (br, phenyl), 5.5, 5.3, and 4.1 (br, m, sugar); IR (KBr, cm^{-1}) 3365 (ν_{O-H}).

Poly(*p*-isocyanophenyl *β*-D-lactoside): $[\alpha]^{25}_D$ −416.9° (*c* 0.5, H_2O); ^{1}H NMR (500 MHz, D_2O, 50 °C) δ 6.7(br, phenyl), 5.5, 5.4, and 4.2 (br, m, sugar); IR (KBr, cm^{-1}) 3345 (ν_{O-H}).

Acknowledgment. This work was supported by the Grant-in-Aid for Scientific Research on Priority Areas from the Ministry of Education, Science and Culture.

References and Notes

(1) *Glycoproteins*; Montreuil, J., Vliegenthart, J. F. G., Schachter, H., Ed.; Elsevier Science B. V.: Amsterdam, 1995; Vol. 29a.
(2) *Molecular Glycobiology*; Fukuda, M., Hindsgaul, O., Ed.; Oxford University Press: Oxford, 1994.
(3) Dwek, R. A. *Biochem. Soc. Trans.* **1994**, *23*, 1−25.
(4) Lee, Y. C. In *Neoglycoconjugates*; Lee, Y. C., Ed.; Academic Press: San Diego, 1994; pp 3−21.
(5) Lee, Y. C.; Lee, R. T. *Acc. Chem. Res.* **1995**, *28*, 321−327.
(6) Mammen, M.; Choi, S.-K.; Whitesides, J. M. *Angew. Chem., Int. Ed.* **1998**, *37*, 2754−2794.
(7) Spaltenstein, A.; Whitesides, G. *J. Am. Chem. Soc.* **1991**, *113*, 686−687.
(8) Matsuoka, K.; Nishimura, S.-I. *Macromalecules* **1995**, *28*, 2961−2968.
(9) Mortell, K. H.; Weatherman, R. V.; Kiessling, L. L. *J. Am. Chem. Soc.* **1996**, *118*, 2297−2298.
(10) Page, D.; Zenini, D.; Roy, R. *Bioorg. Med. Chem.* **1996**, *4*, 1949−1961.
(11) Bovin, N. V.; Gabius, H.-J. *Chem. Soc. Rev.* **1995**, *24*, 413−421.
(12) Kiessling, L. L.; Pohl, N. L. *Chem. Biol.* **1996**, *3*, 71−77.
(13) Kobayashi, K.; Kobayashi, A.; Tobe, S.; Akaike, T. In *Neoglycoconjugates*; Lee, Y. C., Ed.; Academic Press: San Diego, 1994; pp 261−284.
(14) Kobayashi, K.; Tsuchida, A.; Usui, T.; Akaike, T. *Macromolecules* **1997**, *30*, 2016−2020.
(15) Tsuchida, A.; Akimoto, S.; Usui, T.; Kobayashi, K. *J. Biochem.* **1998**, *123*, 715−721.
(16) Wataoka, I.; Urakawa, H.; Kajiwara, K.; Kobayashi, K. *Macromolecules* **1999**, *32*, 1816−1821.
(17) Nolte, R. J. M. *Chem. Soc. Rev.* **1994**, 11−19.
(18) Nolte, R. J. M.; van Zomerern, J. A. J.; Zwikker, J. W. *J. Org. Chem.* **1978**, *43*, 1972−1975.
(19) van der Eijk, J. M.; Nolte, R. J. M.; Drenth, W.; Hezemans, A. M. F. *Macromolecules* **1980**, *13*, 1391−1397.
(20) Visser, H. G. J.; Nolte, R. J. M.; Zwikker, J. W.; Drenth, W. *J. Org. Chem.* **1985**, *50*, 3138−3143.
(21) Roks, M. F. M.; Nolte, R. J. M. *Macromolecules* **1992**, *25*, 5398−5407.
(22) Cornelissen, J. J. L. M.; Fischer, M.; Sommerdijk, N. A. J. M.; Nolte, R. J. M. *Science* **1998**, *280*, 1427−1430.
(23) Deming, T. J.; Novak, B. M. *J. Am. Chem. Soc.* **1993**, *115*, 9101−9111.
(24) Clericuzio, M.; Alagona, G.; Ghio, C.; Salvadori, P. *J. Am. Chem. Soc.* **1997**, *119*, 1059−1071.
(25) van Beijnen, A. J. M.; Nolte, R. J. M.; Zwikker, J. W.; Drenth, W. *J. Mol. Catal.* **1978**, *4*, 427−432.
(26) Sun, H. *J. Comput. Chem* **1994**, *15*, 752−768.
(27) Sun, H.; Mumby, S. J.; Maple, J. R.; Hagler, A. T. *J. Am. Chem. Soc.* **1994**, *116*, 2978−2987.
(28) Sun, H. *Macromolecules* **1995**, *28*, 701−712.
(29) Kobayashi, K.; Kakishita, N.; Okada, M.; Akaike, T.; Usui, T. *J. Carbohydr. Chem.* **1994**, *13*, 753−766.
(30) Goldstein, I. J.; Hayes, C. H. *Adv. Carbohydr. Chem. Biochem.* **1978**, *35*, 127−340.
(31) Lotan, R.; Sharon, N. *Biochem. Biophys. Res. Commun.* **1973**, *55*, 1340−1346.
(32) Privat, J.-P.; Delmotte, F.; Mialonier, G.; Bouchard, P.; Monsigny, M. *Eur. J. Biochem.* **1974**, *47*, 5−14.

MA990444J